nature cell biology

Cdc14 phosphatase promotes segregation of telomeres through repression of RNA polymerase II transcription

Andres Clemente-Blanco[1], Nicholas Sen[1], Maria Mayan-Santos[1], Maria P. Sacristán[2], Bryony Graham[3], Adam Jarmuz[1], Adam Giess[4], Elizabeth Webb[4], Laurence Game[4], Dirk Eick[5], Avelino Bueno[2], Matthias Merkenschlager[3] and Luis Aragón[1,6]

Kinases and phosphatases regulate messenger RNA synthesis through post-translational modification of the carboxy-terminal domain (CTD) of the largest subunit of RNA polymerase II (ref. 1). In yeast, the phosphatase Cdc14 is required for mitotic exit[2,3] and for segregation of repetitive regions[4]. Cdc14 is also a subunit of the silencing complex RENT (refs 5,6), but no roles in transcriptional repression have been described. Here we report that inactivation of Cdc14 causes silencing defects at the intergenic spacer sequences of ribosomal genes during interphase and at Y′ repeats in subtelomeric regions during mitosis. We show that the role of Cdc14 in silencing is independent of the RENT deacetylase subunit Sir2. Instead, Cdc14 acts directly on RNA polymerase II by targeting CTD phosphorylation at Ser 2 and Ser 5. We also find that the role of Cdc14 as a CTD phosphatase is conserved in humans. Finally, telomere segregation defects in *cdc14* mutants[4] correlate with the presence of subtelomeric Y′ elements and can be rescued by transcriptional inhibition of RNA polymerase II.

The conserved Cdc14 (cell division cycle 14) family of phosphatases regulates several key events during late mitosis, most notably they promote reversal of Cdk1-dependent phosphorylation and thus mitotic exit[2,3,5]. In budding yeast, Cdc14 localizes dynamically to different cellular structures in a cell-cycle-dependent manner. During interphase Cdc14 is bound to the nucleolus[6], whereas at anaphase it is released throughout the cell[7]. Two regulatory networks activate Cdc14 during mitosis, FEAR (Cdc fourteen early anaphase release) and MEN (mitotic exit network)[3]. The FEAR activation occurs in early anaphase and is important to coordinate many anaphase events, whereas MEN operates in late anaphase[3]. Cdc14 activation by FEAR is crucial for the faithful execution of many anaphase processes, including timely chromosome segregation. This role was identified through the observation that segregation errors are present in Cdc14 mutants but not MEN mutants[4,8,9]. Interestingly, such defects occur at specific genome regions, namely the repetitive ribosomal DNA (rDNA) gene array and telomeres[4,8,9]. The failure to segregate ribosomal repeats in *cdc14* mutants is caused by a lack of RNA polymerase I (RNAP-I) transcription inhibition[10–12], a process required for the loading of the condensin complex to these repeats during anaphase. In contrast, the role of Cdc14 in telomere segregation is unknown. Importantly, Cdc14 inactivation in cells tricked to transcribe ribosomal genes with RNAP-II, instead of RNAP-I, also causes segregation failure of the ribosomal repeats[11]. Therefore, one hypothesis would be that Cdc14 promotes transcription repression of RNAP-II genes at subtelomeric sites. This possibility is particularly appealing because nucleolar Cdc14 was originally discovered as a subunit of the silencing RENT (regulator of nucleolar silencing and telophase exit) complex[5,6], which inhibits transcription by RNAP-II at the rDNA intergenic spacers (IGS). Besides Cdc14, RENT contains Sir2 and Cfi1 (also known as Net1; refs 5,6). Roles for Sir2 and Cfi1 in rDNA silencing have been described extensively[13–15]; however, a role for Cdc14 in RNAP-II silencing has not been carefully assessed.

Growth assays are available for the examination of transcription silencing within the silenced loci in the yeast genome; however, the contribution of essential genes, such as Cdc14, to silencing cannot be analysed using these methods. To circumvent this limitation, we used quantitative real-time PCR (rtPCR) to measure levels of endogenous transcripts of the IGS regions within yeast ribosomal repeats on chromosome XII (Fig. 1a) in the conditional mutant *cdc14-1* at permissive (25 °C) and non-permissive (37 °C) temperatures. An increase in the number of IGS transcripts was observed in *cdc14-1* mutants at 37 °C (relative to 25 °C), but not in wild-type cells (Fig. 1b,c). To determine whether the effect of Cdc14 on IGS

[1]Cell Cycle Group, MRC Clinical Sciences Centre, Imperial College, Du Cane Road, London W12 ONN, UK. [2]Centro de Investigación del Cáncer, Universidad de Salamanca/CSIC, 37007 Salamanca, Spain. [3]Lymphocyte Development Group, MRC Clinical Sciences Centre, Imperial College, Du Cane Road, London W12 ONN, UK. [4]Genomics Laboratory, MRC Clinical Sciences Centre, Imperial College, Du Cane Road, London W12 ONN, UK. [5]Department of Molecular Epigenetics, Helmholtz-Center Munich, Center of Integrated Protein Science (CIPSM), Marchioninistrasse 25, 81377 Munich, Germany.
[6]Correspondence should be addressed to L.A. (e-mail: luis.aragon@csc.mrc.ac.uk)

Received 22 June 2011; accepted 22 September 2011; published online 23 October 2011; DOI: 10.1038/ncb2365

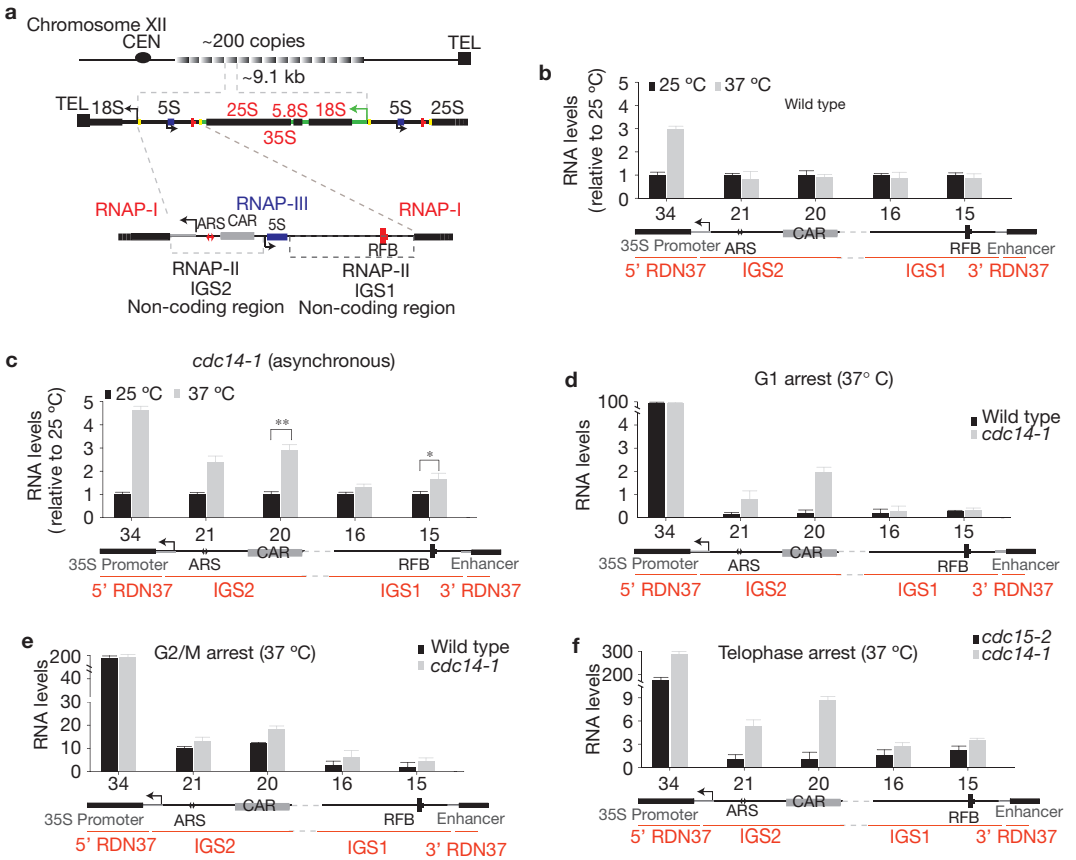

Figure 1 Cdc14 is required for rDNA silencing. (**a**) Schematic representation of the intergenic spacer regions (IGS1/IGS2). Specific features of these regions include a replication origin (ARS), a cohesin binding site (CAR) and a replication fork barrier sequence (RFB). (**b**) rtPCR-based analysis of transcripts within IGS regions in wild-type cells grown at 25 °C and 37 °C. Transcription levels relative to 25 °C are shown for each position (mean ± s.e.m., $n = 3$). (**c**) rtPCR-based analysis of transcripts within IGS regions in *cdc14-1* cells grown at 25 °C and 37 °C. Transcription levels relative to 25 °C are shown for each position (mean ± s.e.m., $n = 7$). *P* values: *0.016, **0.005; Student's *t*-test. (**d**) rtPCR-based analysis of transcripts within IGS regions in wild-type and *cdc14-1* cells arrested in G1 at 25 °C (with α-factor) and shifted to 37 °C for two additional hours (mean ± s.e.m., $n = 3$). (**e**) rtPCR-based analysis of transcripts within IGS regions in wild-type and *cdc14-1* cells arrested in metaphase at 25 °C (with nocodazole) and shifted to 37 °C (mean ± s.e.m., $n = 3$). (**f**) rtPCR-based analysis of transcripts within IGS regions in *cdc15-2* and *cdc14-1* cells grown at 25 °C and shifted to 37 °C for three hours to reach a telophase arrest (mean ± s.e.m., $n = 3$).

transcription is independent of its role in mitotic exit during anaphase, we measured total IGS transcription in *cdc14-1* and wild-type cells blocked in G1 and G2/M at 37 °C. An increase in the number of IGS transcripts, particularly at IGS2, was observed for *cdc14-1* cells in these arrests (Fig. 1d,e).

In *cdc14-1* mutant cells, exit from mitosis is prevented under non-permissive conditions leading to cell cycle arrest in telophase. To ensure that the increased level of IGS transcription observed (Fig. 1b–d) is not due to the cell cycle arrest, we compared *cdc14-1* to *cdc15-2* mutants, which also arrest in telophase. Importantly, Cdc14 is bound to IGS regions in the final telophase arrest by *cdc15-2* inactivation[7], which provides an ideal control for a telophase arrest with Cdc14 bound to IGS regions. A similar increase in the number of IGS transcripts was observed in the *cdc14-1* anaphase arrest relative to *cdc15-2* cells (Fig. 1f). These results confirm that, similarly to other RENT members, Cdc14 contributes to rDNA silencing. Therefore, Cdc14 plays a role in rDNA silencing independent of its main cell cycle function during anaphase.

Sir2 is an NAD-dependent deacetylase that targets histone H3 and H4 to promote rDNA silencing[16]. It is possible that the role of Cdc14 in rDNA silencing (Fig. 1b–e) is fully mediated by Sir2 function. To examine this, we first investigated whether Sir2 localizes to IGS regions in the absence of Cdc14. We found that Cdc14 inactivation decreased the level of Sir2 binding across IGS (Fig. 2a). Next, we investigated whether Cdc14 inactivation affected rDNA silencing in the absence of Sir2. We found an increased IGS transcription level in double-mutant cells (*sir2*Δ *cdc14-1*) when compared with single mutants (Fig. 2b), demonstrating that in the absence of Sir2, Cdc14 supports silencing at IGS regions.

In addition to silencing, transcription of non-coding RNA within the IGS regions is also subject to degradation, a process mediated by the TRAMP (Trf4–Air2–Mtr4p polyadenylation) complex and by the exosome[17]. Next we investigated whether the increased level of IGS transcription in *cdc14-1* cells is caused by defects of this degradation pathway. We deleted Trf4, the poly(A) polymerase component of TRAMP4, in *cdc14-1* cells and investigated IGS transcription in the presence and absence of Cdc14 (Fig. 2c). Double-mutant *trf4*Δ *cdc14-1* cells showed an increase in IGS transcription when compared with single mutants (Fig. 2c), which demonstrates that elevated IGS transcription in *cdc14-1* cells is not caused by defects in TRAMP-mediated degradation of non-coding RNA.

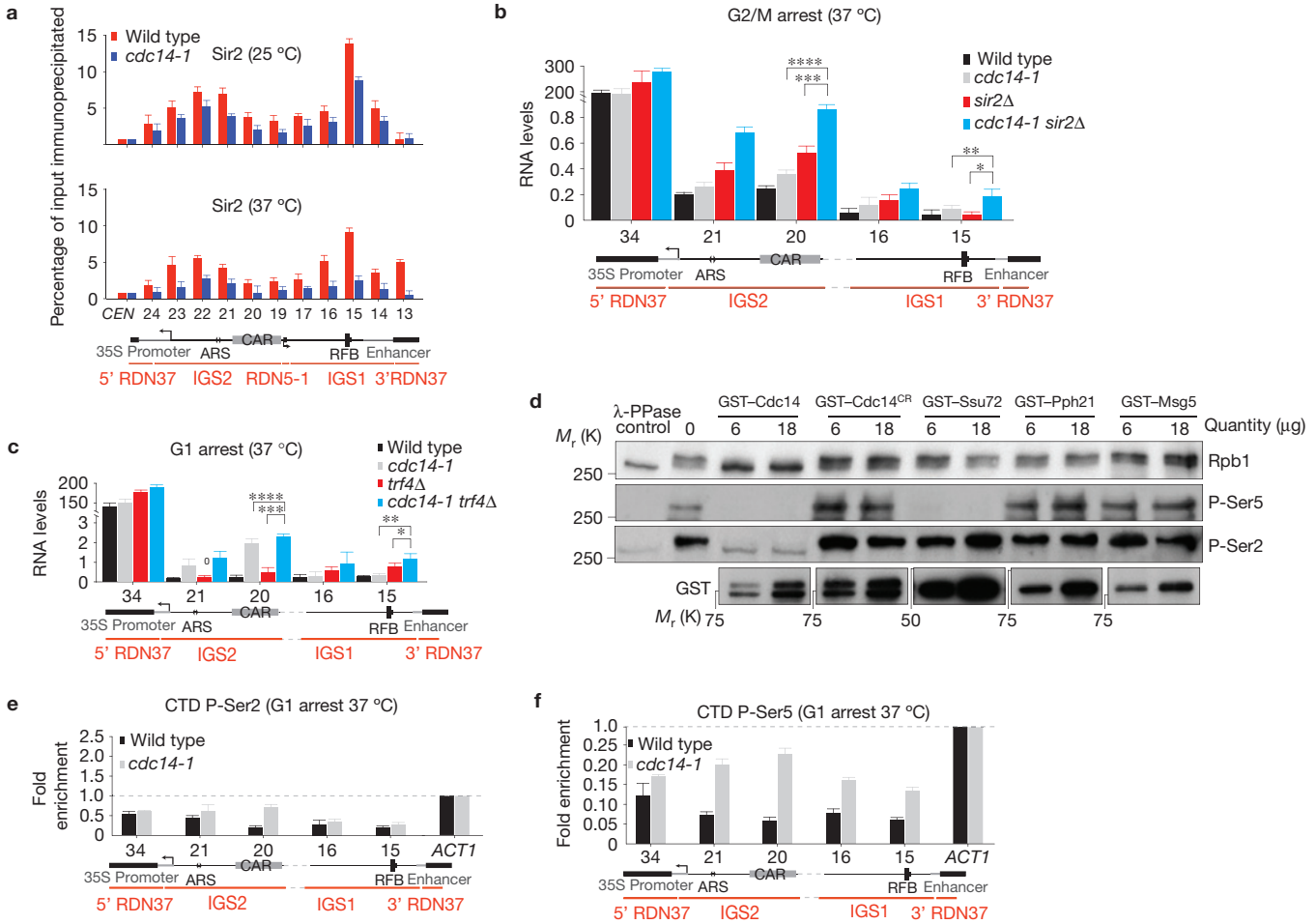

Figure 2 Cdc14 is an RNAP-II CTD phosphatase. (**a**) ChIP analysis of Sir2 binding at 25 °C (top) and 37 °C (bottom) in *cdc14-1* and wild-type cells within the rDNA IGS regions of chromosome XII. Fold enrichment relative to *CEN4* is shown for each location (mean ± s.e.m., $n = 4$). (**b**) rtPCR-based analysis of transcripts within IGS regions in wild-type, *sir2*Δ, *cdc14-1* and *sir2*Δ *cdc14-1* cells arrested in metaphase at 25 °C (with nocodazole) and shifted to 37 °C for two additional hours (mean ± s.e.m., $n = 8$). *P* values: *0.036, **0.047, ***0.016, ****0.021; Student's *t*-test. (**c**) rtPCR-based analysis of transcripts within IGS regions in wild-type, *trf4*Δ, *cdc14-1* and *trf4*Δ *cdc14-1* cells arrested in G1 at 25 °C (with α-factor) and shifted to 37 °C for two additional hours (mean ± s.e.m., $n = 8$). *P* values: *0.031, **0.028, ***0.020, ****0.051; Student's *t*-test. (**d**) Purified Rpb1 was incubated with buffer, purified GST–Cdc14, a catalytically inactive mutant GST–Cdc14^{CR} (C283S, R289A), GST–Ssu72, GST–Pph21 or GST–Msg5, then analysed by immunoblotting using antibodies against CTD Ser 5 and Ser 2 phosphorylation. The quantity (μg) of purified protein added to each reaction is shown. (**e**) ChIP analysis of RNAP-II phosphorylated at CTD Ser 2 (P-Ser2) within IGS regions in wild-type and *cdc14-1* cells arrested in G1 at 25 °C (with α-factor) and shifted to 37 °C for two additional hours. Fold enrichment relative to the *ACT1* locus is shown (mean ± s.e.m., $n = 3$). (**f**) ChIP analysis of RNAP-II phosphorylated at CTD Ser 5 (P-Ser5) within IGS regions in wild-type and *cdc14-1* cells arrested in G1 at 25 °C (with α-factor) and shifted to 37 °C for two additional hours. Fold enrichment relative to the *ACT1* locus is shown (mean ± s.e.m., $n = 3$). Uncropped images of blots are shown in Supplementary Fig. S4.

The transcription activity of RNAP-II is regulated through phosphorylation of the CTD of the core subunit Rpb1 (ref. 18). CTD contains tandem repeats of the heptapeptide, Tyr-Ser-Pro-Thr-Ser-Pro-Ser (Tyr1-Ser2-Pro3-Thr4-Ser5-Pro6-Ser7; ref. 18). RNAP-II recruitment to promoters requires CTD to be hypo-phosphorylated; however, transcription initiation involves phosphorylation on the Ser-5 residues (P-Ser5) of CTD, and elongation on Ser 2 (P-Ser2; ref. 18). Although RNAP-II has been shown to bind to IGS regions, it does not elongate[19], and thus the regions are silenced[13–15].

As Cdc14 is a proline-directed phosphatase and both Ser 2 and Ser 5 residues on the CTD are followed by proline, we explored whether these CTD residues are a substrate of Cdc14. We incubated purified Cdc14 (GST–Cdc14), expressed in bacterial cells, with Rpb1 extracted from yeast. In the absence of Cdc14, Rpb1 phosphorylation was detected on both Ser 2 and Ser 5 (Fig. 2d). Phosphorylation at both Ser 2 and Ser 5 was rapidly and completely lost after incubation with Cdc14 (Fig. 2d). To confirm Cdc14 specificity in the *in vitro* phosphatase assay, several controls were also carried out. Rpb1 incubation with a phosphatase-inactive Cdc14 (GST–Cdc14^{CR}; ref. 20), the PP2A catalytic subunit Pph21 (ref. 21) or the dual-specificity protein phosphatase (DSP) Msg5 (ref. 22) did not affect Ser 5 or Ser 2 phosphorylation (Fig. 2d). In contrast, incubation with the CTD Ser 5 phosphatase Ssu72 (ref. 23) led to loss of Ser 5 but not Ser 2 phosphorylation (Fig. 2d). *In vivo*, Cdc14 activity as a CTD phosphatase was consistent with an observed increase in the level of CTD Ser 5 and Ser 2 phosphorylation on the IGS region following Cdc14 inactivation (Fig. 2e,f).

Our findings demonstrate that Cdc14 binding to IGS regions in interphase contributes to their silencing (Fig. 1). Although Cdc14

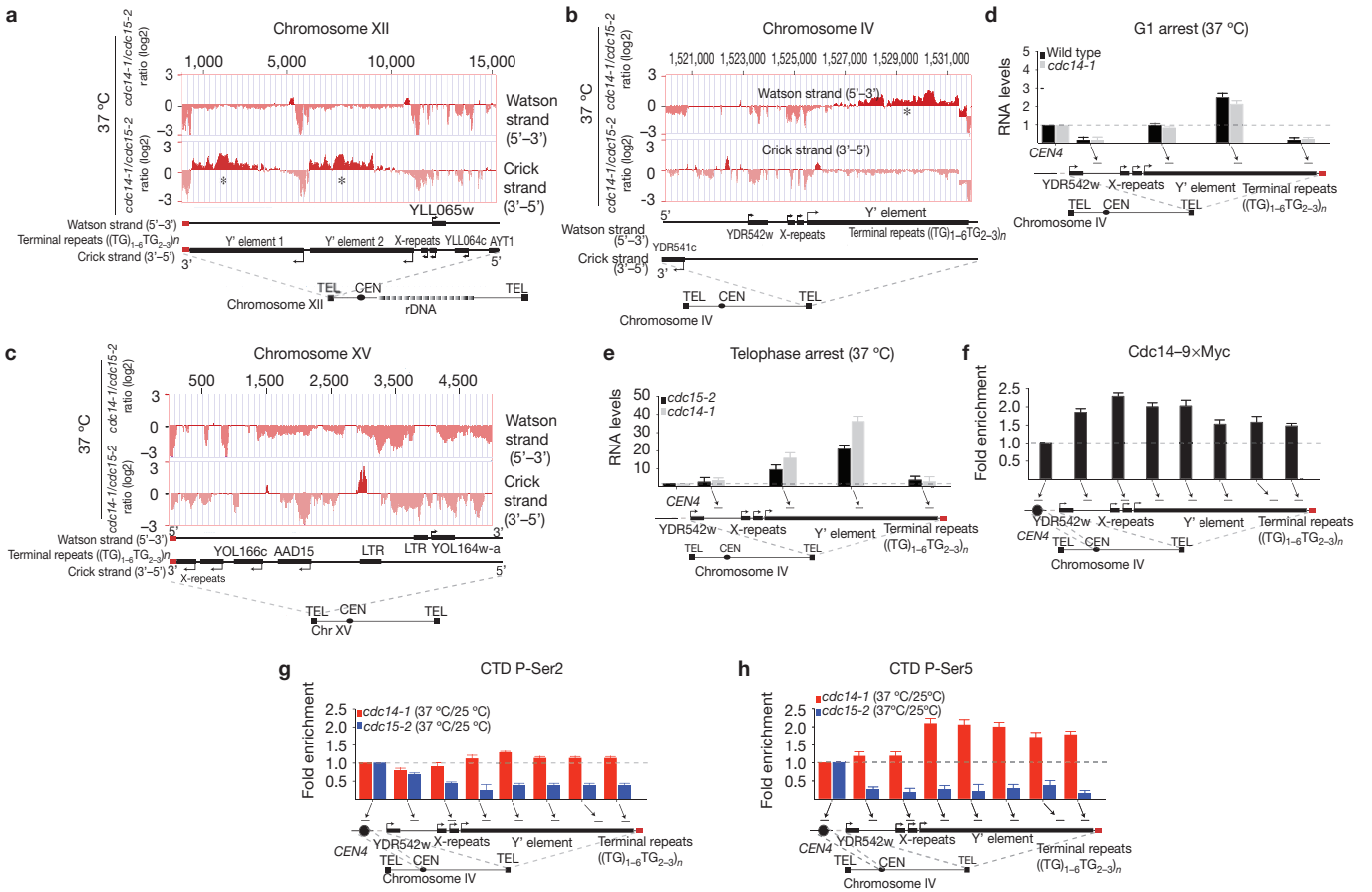

Figure 3 Cdc14 represses transcription of subtelomeric Y′ elements. (**a**) Yeast tiling array intensities of the distal 15 kb of the left telomere of chromosome XII containing two Y′ elements (*x* axis). Plotted is the $\log_2$ ratio of transcript abundance in *cdc14-1* relative to *cdc15-2* cells (red) at 37 °C for the Watson and Crick strands (*y* axis). Y′ elements are indicated (*). Transcript abundance for this region at 25 °C can be found in Supplementary Fig S3. (**b**) Yeast tiling array intensities as in **a** for the distal 10 kb of the right telomere region of chromosome IV. Y′ elements are indicated (*). (**c**) Yeast tiling array intensities as in **a** for the distal 5 kb of the left telomere region of chromosome XV. The region does not contain Y′ elements. Transcript abundance for this region at 25 °C can be found in Supplementary Fig S2. (**d**) rtPCR-based analysis of transcripts within the region of the right telomere of chromosome IV in wild-type and *cdc14-1* cells arrested in G1 at 25 °C (with α-factor) and shifted to 37 °C or maintained at 25 °C for two additional hours. RNA levels relative to *CEN4* are shown for each position (mean ± s.e.m., $n = 3$). (**e**) rtPCR-based analysis of transcripts within the region of the right telomere of chromosome IV in *cdc15-2* and *cdc14-1* cells grown at 25 °C and shifted to 37 °C for three hours to reach a telophase arrest. RNA levels relative to *CEN4* are shown for each position (mean ± s.e.m., $n = 3$). (**f**) ChIP analysis of Cdc14 binding within the subtelomeric region of the right telomere of chromosome IV. Fold enrichment relative to *CEN4* is shown for each position (mean ± s.e.m., $n = 3$). (**g**) ChIP analysis of CTD Ser 2 phosphorylation (P-Ser2) at 37 °C relative to 25 °C in *cdc14-1* and *cdc15-2* cells within the subtelomeric region of the right telomere of chromosome IV. Fold enrichment relative to *CEN4* is shown for each position (mean ± s.e.m., $n = 3$). (**h**) ChIP analysis of CTD Ser 5 phosphorylation (P-Ser5) as in **g**. Fold enrichment relative to *CEN4* is shown for each position (mean ± s.e.m., $n = 3$).

is confined to rDNA during interphase, it is released from the nucleolus during anaphase through the sequential activation of the FEAR and MEN regulatory networks[3]. Next, we sought to determine whether the release of Cdc14 during anaphase affects transcription of RNAP-II genes outside rDNA. To investigate this, we compared transcription profiles on genome-wide strand-specific tiling arrays[24] in *cdc14-1* and *cdc15-2* arrested cells. Comparison of *cdc14-1* and *cdc15-2* transcription in the arrays across the IGS regions confirmed the increase in the level of IGS transcription previously observed for *cdc14-1* cells (Supplementary Fig. S1). Next, we looked for regions that showed an increase in the level of transcription in *cdc14-1* relative to *cdc15-2* cells. We found no significant changes in the profiles of *cdc14-1* and *cdc15-2* arrests genome-wide (data not shown), with the exception of subtelomeric regions that contained Y′ elements. Strikingly, all telomeres containing Y′ elements showed an increase in the level of transcription in *cdc14-1* relative to *cdc15-2* cells (Fig. 3a,b and Supplementary Figs S2 and S3). In contrast, transcription profiles of telomeres lacking Y′ elements were identical in *cdc14-1* and *cdc15-2* cells (Fig. 3c). We observed these Cdc14-dependent transcription changes in Y′ elements to occur specifically during anaphase (Fig. 3d,e). Supporting these data, we found that Cdc14 is enriched on the Y′ element of the right arm of chromosome IV (*TEL4R*-Y′; Fig. 3f) and that the level of CTD phosphorylation increased in the absence of Cdc14 activity in this region (Fig. 3g,h).

In budding yeast, Cdc14 is required for the segregation of repetitive regions, mainly the ribosomal gene array[4,8,9] (rDNA) and telomeres[4]. The rDNA non-disjunction phenotype observed in *cdc14-1* cells stems from a defect in repressing transcription of ribosomal genes[10–12], which is a requirement for condensin recruitment to rDNA (refs 4,25) and

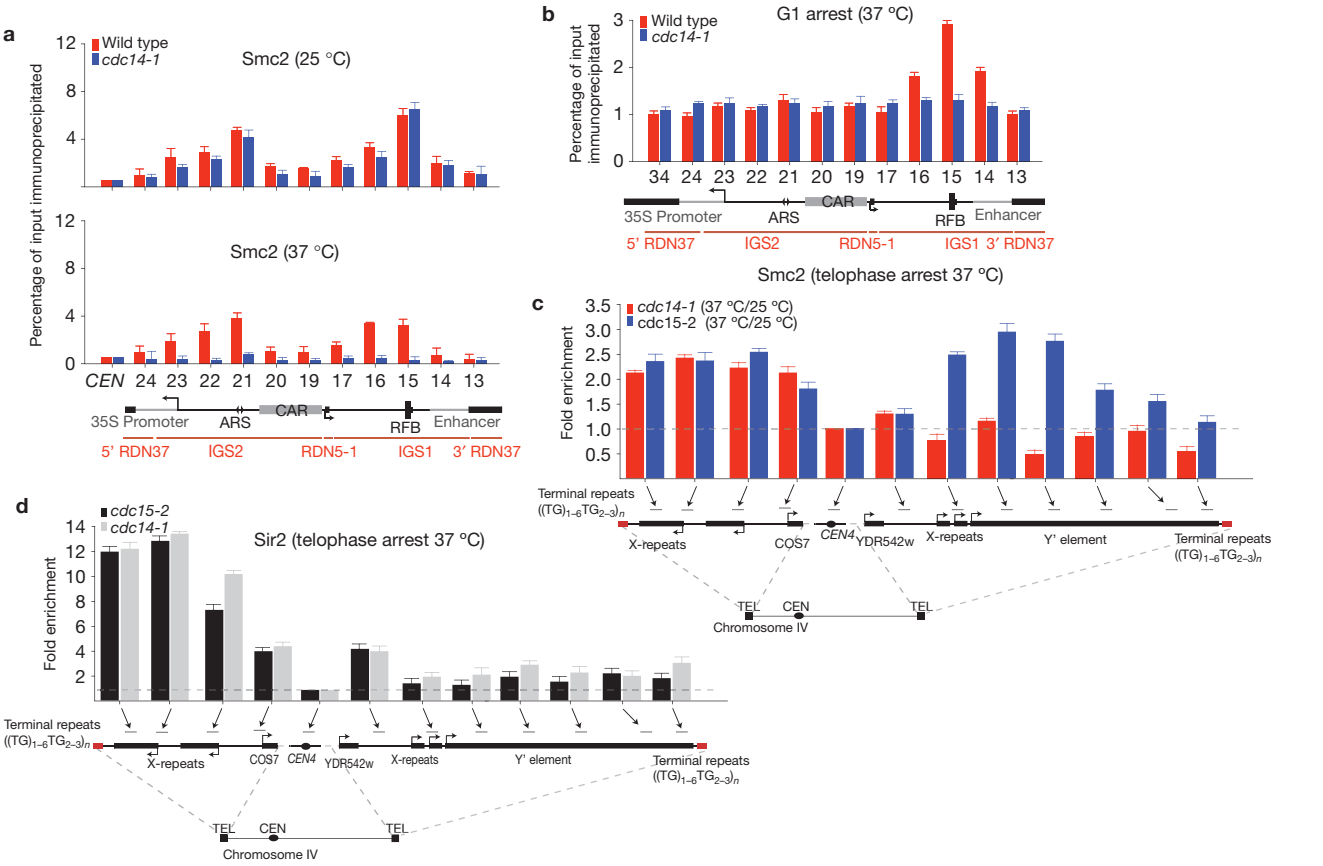

Figure 4 Cdc14 recruits condensin to telomeres containing Y′ elements. (**a**) ChIP analysis of Smc2 binding at 25 °C (top) and 37 °C (bottom) in *cdc14-1* and wild-type cells within the rDNA IGS regions of chromosome XII. Fold enrichment relative to *CEN4* is shown for each location (mean ± s.e.m., $n = 3$). (**b**) ChIP analysis of condensin subunit Smc2 binding within IGS regions in wild-type and *cdc14-1* cells arrested in G1 at 25 °C (with α-factor) and shifted to 37 °C for two additional hours. Data are shown as a percentage of input immunoprecipitated for each position (mean ± s.e.m., $n = 4$). (**c**) ChIP analysis of condensin subunit Smc2 binding at 37 °C relative to 25 °C in *cdc14-1* and *cdc15-2* cells within the subtelomeric (left, *TEL4L*, and right, *TEL4R*, arms) and centromeric (*CEN4*) regions of chromosome IV. Fold enrichment relative to *CEN4* is shown for each position (mean ± s.e.m., $n = 3$). (**d**) ChIP analysis of Sir2 binding at 37 °C relative to 25 °C in *cdc14-1* and *cdc15-2* cells within the *TEL4L*, *CEN4* and *TEL4R* regions of chromosome IV. Fold enrichment relative to *CEN4* is shown for each location (mean ± s.e.m., $n = 3$).

anaphase disjunction of the locus[26]. Next, we sought to determine whether condensin binds to the subtelomeric Y′ element on *TEL4R* in a Cdc14-dependent manner during anaphase. We compared binding of condensin subunit Smc2 in *cdc14-1* cells on the rDNA IGS and *TEL4R*-Y′ regions (Fig. 4a,b). Consistent with previous reports, we observed that the level of condensin binding to rDNA is decreased in the absence of Cdc14 (refs 4,25; Fig. 4a). We note that the Smc2 binding profile in G1-arrested cells showed accumulation on *IGS1* but not *IGS2* (Fig. 4b). At present, we do not know the exact reason for this; however, condensin has recently been shown to form a ring that topologically entraps DNA (ref. 27); therefore, it is possible that, as in the case of cohesin[28], the transcription machinery can slide condensin through the template. Next, we investigated the effect of Cdc14 on condensin binding to telomeric regions during anaphase. We found that whereas Smc2 binds to both the left and right telomeric regions of chromosome IV (*TEL4L*, lacking Y′ elements, and *TEL4R*-Y′) in *cdc15-2* arrests (Fig. 4c), it binds to *TEL4L* but not *TEL4R*-Y′ in *cdc14-1* arrested cells (Fig. 4c). This result demonstrates that Smc2 binds to subtelomeric Y′ elements in a Cdc14-dependent manner during anaphase. Unlike condensin, Sir2 binding on *TEL4R*-Y′ was unaffected by Cdc14 inactivation (Fig. 4d). Therefore, the Cdc14 function at telomeric Y′ elements is independent of Sir2. Recent reports demonstrated that the related rDNA structural complex cohibin has a Sir2-dependent role in telomere silencing and stability[29]. This may be evidence for a division of labour in genome maintenance between closely related complexes.

The lack of condensin binding to *TEL4R*-Y′ but not *TEL4L* in *cdc14-1* arrests prompted us to investigate the segregation of chromosome IV in these arrests. We introduced arrays of *tet* operators (*tetO*), to visualize chromosome regions (chromosome dots), at different positions on this chromosome: at centromere proximal regions (*CEN4* dot; 150 kilobases (kb) away from *CEN4*), the left telomere (*TEL4L* dot; 30 kb away from *TEL4L*), the right telomere (*TEL4R* dot; 30 kb away from *TEL4R*) and two interstitial sites on the right arm (*ARM1* dot and *ARM2* dot; Fig. 5a). We found that *TEL4L* dots and *CEN4* dots were fully segregated in the *cdc14-1* arrest whereas *TEL4R* dots did not separate despite evident segregation of nuclear masses (Fig. 5a,b). An intermediate degree of segregation was observed for the *ARM* dots (Fig. 5a). We note that the *TEL4R* dot segregation failure was characterized by the presence of a single GFP dot in one of the segregated nuclei (Fig. 5b). There are two potential interpretations for this phenotype. One possibility is that replication of telomeric regions containing Y′ elements is incomplete,

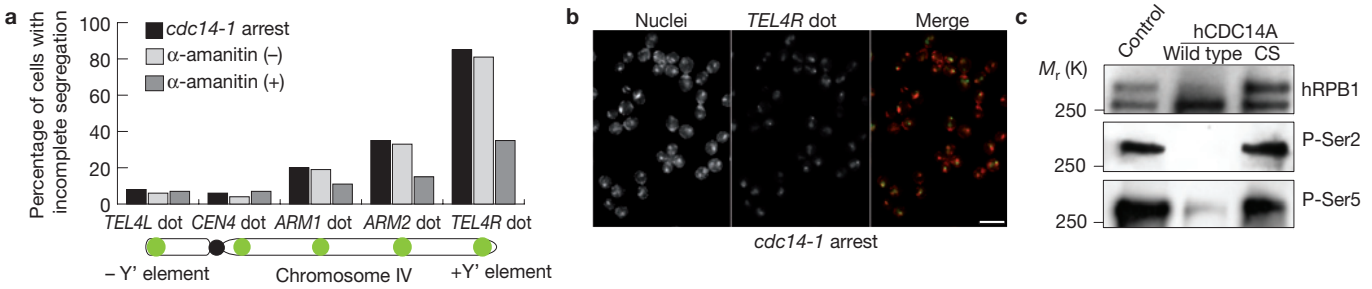

Figure 5 Segregation of telomeres with Y′-elements requires Cdc14. (**a**) Segregation analysis of *cdc14-1* mutant strains carrying a *tetO* dot close to *CEN4* (*CEN4* dot), the left telomere (*TEL4L* dot), the right telomere (*TEL4R* dot) or the middle of chromosome IV (*ARM1* dot and *ARM2* dot; as indicated). Cells were released from G1 (α-factor) into telophase arrest at 37 °C (*cdc14-1* arrest), before treatment with the RNAP-II inhibitor α-amanitin (66 μg ml^{-1}). Segregation of *tetO* dots in the arrest (*cdc14-1* arrest) and after α-amanitin (RNAP-II negative) or mock treatment (RNAP-II positive) was scored and quantified (three hundred cells were scored). (**b**) Comparative micrographs showing lack of segregation of *TEL4R* dots in the *cdc14-1* telophase arrest. Scale bar, 10 μm. (**c**) Purified human RPB1 was incubated with hCDC14A or hCDC14A^{CS} (phosphatase-dead) proteins purified from bacterial cells. Western blot analysis of CTD P-Ser2 and P-Ser5 after incubation is shown. Uncropped images of blots are shown in Supplementary Fig. S4.

because Cdc14 has recently been implicated in replication termination at the rDNA (ref. 30). The second possibility, and more likely, is that the lack of condensin loading at these regions (Fig. 4b) prevents resolution of intertwines between sister chromatids[31,32].

To determine whether the telomeric segregation defects in *cdc14-1* cells were caused by transcription of Y′ elements, we used α-amanitin, an RNAP-II specific inhibitor[33], to block RNAP-II transcription. Addition of the drug improved significantly the degree of separation of the *ARM* and *TEL4R* dots (Fig. 5a). Therefore, telomere segregation defects in *cdc14-1* mutants correlate with the presence of Y′ elements in subtelomeric regions and active RNAP-II transcription.

Cdc14 is a highly conserved phosphatase. In the human genome, two Cdc14 homologues have been identified, hCDC14A and hCDC14B. CDC14A causes mitotic CDK inactivation[34], and its depletion by RNA-mediated interference (RNAi) leads to centrosome duplication, mitotic and cytokinesis defects[35], supporting a role in chromosome partitioning and genome stability. It is differentially expressed in human cancer cells, interacts with the Cdk1–cyclin-B complex and p53 (ref. 36), and exhibits cytoplasmic localization during interphase[37]. In contrast, CDC14B, similarly to yeast Cdc14, localizes to the nucleolus in interphase but not during mitosis[37]. Recent studies have linked CDC14B to the DNA-damage checkpoint response during the G2 stage of the cell cycle[38]. The role of Cdc14 as an RNAP-II phosphatase in yeast prompted us to investigate whether this is an evolutionarily conserved function. We expressed and purified the human Cdc14 homologue hCDC14A from bacterial cells and investigated its phosphatase activity *in vitro* on human hRPB1 purified from HEK293T cells. Incubation of hRPB1 with purified hCDC14A led to the loss of Ser 2 and Ser 5 phosphorylation (Fig. 5c).

Our study identifies a previously unknown and conserved role for the mitotic exit phosphatase Cdc14 in the repression of RNAP-II transcription in repetitive regions of the yeast genome. Moreover, Cdc14 function links RNAP-II and chromosome segregation through the evidence that transcriptional repression of subtelomeric regions containing Y′ elements by Cdc14 facilitates condensin loading to and segregation of these telomeres. We propose that mitotic RNAP-II transcription inhibition facilitates loading of factors that mediate structural functions on mitotic chromosomes. □

METHODS

Methods and any associated references are available in the online version of the paper at http://www.nature.com/naturecellbiology

Note: Supplementary Information is available on the Nature Cell Biology website

ACKNOWLEDGEMENTS

We are very grateful to L. Warfield and S. Hahn for advice. We thank D. Morgan (UCSF) and A. Amon (MIT) for reagents. We are grateful to all members of the Aragon laboratory for discussions and comments on the manuscript. The Bueno and Sacristán laboratories are financially supported by grants from the Spanish Science Ministry (MICINN). The Eick laboratory is supported by the Deutsche Forschungsgemeinschaft, SFB-Transregio5. The Aragon and Merkenschlager laboratories are supported by the Medical Research Council (MRC) of the UK.

AUTHOR CONTRIBUTIONS

A.C-B. and L.A. conceived the study and analysed the data with critical input from M.M. Experiments were conducted by A.C-B., N.S., M.M-S., A.J. and B.G. Microarray analysis was done by L.G. A.G. and E.W. Critical materials were provided by M.P.S., A.B. and D.E. L.A. wrote the paper and all authors discussed the results and commented on the manuscript.

COMPETING FINANCIAL INTERESTS

The authors declare no competing financial interests.

Published online at http://www.nature.com/naturecellbiology
Reprints and permissions information is available online at http://www.nature.com/reprints

1. Orphanides, G. & Reinberg, D. A unified theory of gene expression. *Cell* **108,** 439–451 (2002).
2. Visintin, R. *et al.* The phosphatase Cdc14 triggers mitotic exit by reversal of Cdk-dependent phosphorylation. *Mol. Cell.* **2,** 709–718 (1998).
3. Stegmeier, F. & Amon, A. Closing mitosis: the functions of the Cdc14 phosphatase and its regulation. *Annu. Rev. Genet.* **38,** 203–232 (2004).
4. D'Amours, D., Stegmeier, F. & Amon, A. Cdc14 and condensin control the dissolution of cohesin-independent chromosome linkages at repeated DNA. *Cell* **117,** 455–469 (2004).
5. Shou, W. *et al.* Exit from mitosis is triggered by Tem1-dependent release of the protein phosphatase Cdc14 from nucleolar RENT complex. *Cell* **97,** 233–244 (1999).
6. Visintin, R., Hwang, E. S. & Amon, A. Cfi1 prevents premature exit from mitosis by anchoring Cdc14 phosphatase in the nucleolus. *Nature* **398,** 818–823 (1999).
7. Stegmeier, F., Visintin, R. & Amon, A. Separase, polo kinase, the kinetochore protein Slk19, and Spo12 function in a network that controls Cdc14 localization during early anaphase. *Cell* **108,** 207–220 (2002).
8. Torres-Rosell, J., Machin, F., Jarmuz, A. & Aragon, L. Nucleolar segregation lags behind the rest of the genome and requires Cdc14p activation by the FEAR network. *Cell Cycle* **3,** 496–502 (2004).

9. Sullivan, M., Higuchi, T., Katis, V. L. & Uhlmann, F. Cdc14 phosphatase induces rDNA condensation and resolves cohesin-independent cohesion during budding yeast anaphase. *Cell* **117,** 471–482 (2004).
10. Machin, F. *et al.* Transcription of ribosomal genes can cause nondisjunction. *J. Cell Biol.* **173,** 893–903 (2006).
11. Tomson, B. N., D'Amours, D., Adamson, B. S., Aragon, L. & Amon, A. Ribosomal DNA transcription-dependent processes interfere with chromosome segregation. *Mol. Cell. Biol.* **26,** 6239–6247 (2006).
12. Clemente-Blanco, A. *et al.* Cdc14 inhibits transcription by RNA polymerase I during anaphase. *Nature* **458,** 219–222 (2009).
13. Smith, J. S. & Boeke, J. D. An unusual form of transcriptional silencing in yeast ribosomal DNA. *Genes Dev.* **11,** 241–254 (1997).
14. Bryk, M. *et al.* Transcriptional silencing of Ty1 elements in the RDN1 locus of yeast. *Genes Dev.* **11,** 255–269 (1997).
15. Straight, A. F. *et al.* Net1, a Sir2-associated nucleolar protein required for rDNA silencing and nucleolar integrity. *Cell* **97,** 245–256 (1999).
16. Imai, S. *et al.* Sir2: an NAD-dependent histone deacetylase that connects chromatin silencing, metabolism, and aging. *Cold Spring Harb. Symp. Quant. Biol.* **65,** 297–302 (2000).
17. Houseley, J., Kotovic, K., El Hage, A. & Tollervey, D. Trf4 targets ncRNAs from telomeric and rDNA spacer regions and functions in rDNA copy number control. *EMBO J.* **26,** 4996–5006 (2007).
18. Egloff, S. & Murphy, S. Cracking the RNA polymerase II CTD code. *Trends Genet.* **24,** 280–288 (2008).
19. Mayan, M. & Aragon, L. Cis-interactions between non-coding ribosomal spacers dependent on RNAP-II separate RNAP-I and RNAP-III transcription domains. *Cell Cycle* **9,** 4328–4337 (2010).
20. Jaspersen, S. L. & Morgan, D. O. Cdc14 activates cdc15 to promote mitotic exit in budding yeast. *Curr. Biol.* **10,** 615–618 (2000).
21. Jiang, Y. Regulation of the cell cycle by protein phosphatase 2A in *Saccharomyces cerevisiae*. *Microbiol. Mol. Biol. Rev.* **70,** 440–449 (2006).
22. Doi, K. *et al.* MSG5, a novel protein phosphatase promotes adaptation to pheromone response in *S. cerevisiae*. *EMBO J.* **13,** 61–70 (1994).
23. Krishnamurthy, S., He, X., Reyes-Reyes, M., Moore, C. & Hampsey, M. Ssu72 is an RNA polymerase II CTD phosphatase. *Mol. Cell* **14,** 387–394 (2004).
24. David, L. *et al.* A high-resolution map of transcription in the yeast genome. *Proc. Natl Acad. Sci. USA* **103,** 5320–5325 (2006).
25. Wang, B. D., Butylin, P. & Strunnikov, A. Condensin function in mitotic nucleolar segregation is regulated by rDNA transcription. *Cell Cycle* **5,** 2260–2267 (2006).
26. Freeman, L., Aragon-Alcaide, L. & Strunnikov, A. The condensin complex governs chromosome condensation and mitotic transmission of rDNA. *J. Cell Biol.* **149,** 811–824 (2000).
27. Cuylen, S., Metz, J. & Haering, C. H. Condensin structures chromosomal DNA through topological links. *Nat. Struct. Mol. Biol.* **18,** 894–901 (2011).
28. Lengronne, A. *et al.* Cohesin relocation from sites of chromosomal loading to places of convergent transcription. *Nature* **430,** 573–578 (2004).
29. Chan, J. N. *et al.* Perinuclear cohibin complexes maintain replicative life span via roles at distinct silent chromatin domains. *Dev. Cell* **20,** 867–879 (2011).
30. Dulev, S. *et al.* Essential global role of CDC14 in DNA synthesis revealed by chromosome underreplication unrecognized by checkpoints in cdc14 mutants. *Proc. Natl Acad. Sci. USA* **106,** 14466–14471 (2009).
31. D'Ambrosio, C., Kelly, G., Shirahige, K. & Uhlmann, F. Condensin-dependent rDNA decatenation introduces a temporal pattern to chromosome segregation. *Curr. Biol.* **18,** 1084–1089 (2008).
32. Baxter, J. *et al.* Positive supercoiling of mitotic DNA drives decatenation by topoisomerase II in eukaryotes. *Science* **331,** 1328–1332 (2011).
33. Chafin, D. R., Guo, H. & Price, D. H. Action of α-amanitin during pyrophosphorolysis and elongation by RNA polymerase II. *J. Biol. Chem.* **270,** 19114–19119 (1995).
34. Bembenek, J & Yu, H Regulation of the anaphase-promoting complex by the dual specificity phosphatase human Cdc14a. *J. Biol. Chem.* **276,** 48237–48242 (2001).
35. Mailand, N. *et al.* Deregulated human Cdc14A phosphatase disrupts centrosome separation and chromosome segregation. *Nat. Cell Biol.* **4,** 317–322 (2002).
36. Paulsen, M. T. *et al.* The p53-targeting human phosphatase hCdc14A interacts with the Cdk1/cyclin B complex and is differentially expressed in human cancers. *Mol. Cancer* **5,** 25 (2006).
37. Kaiser, B. K., Zimmerman, Z. A., Charbonneau, H. & Jackson, P. K. Disruption of centrosome structure, chromosome segregation, and cytokinesis by misexpression of human Cdc14A phosphatase. *Mol. Biol. Cell* **13,** 2289–2300 (2002).
38. Bassermann, F. *et al.* The Cdc14B-Cdh1-Plk1 axis controls the G2 DNA-damage-response checkpoint. *Cell* **134,** 256–267 (2008).

DOI: 10.1038/ncb2365

METHODS

Strains and materials. All relevant yeast strains used are shown in Supplementary Table S1. C-terminal epitope tagging of proteins was carried out using PCR allele replacement methods. Anti-Myc 9E10 monoclonal antibody and anti-HA 12CA5 monoclonal antibody were used (Roche). Cells were collected from exponentially growing cultures at different temperatures or with different sugar sources, depending of the strains used, and stored at −80 °C. The GST–Cdc14 and GST–Cdc14 phosphatase-dead mutant (*CDC14*$^{C283S/R289}$; Cdc14^{CS}), as well as yeast strains expressing Cdc14 from the *GAL1-10* promoter, were gifts from A. Amon (MIT, USA) and D. Morgan (University of California San Francisco, USA). Constructs to target 5.6 kb of *tetO* arrays to different sites on the long arm of chromosome IV were generated by gene synthesis. Chromosome tags were inserted adjacent to *COS7* (*TEL4L* dot), *RAD55* (*CEN4* dot), *ARS430* (*ARM1* dot), *PRP3* (*ARM2* dot) and *IRC4* (*TEL4R* dot) loci. Details are available on request. Tag integrations were confirmed by PCR.

Cell cycle experiments. Cells arrested in G1 were treated with α-factor. To release cells from the α-factor block, we transferred them to fresh media plus pronase E (0.1 mg ml^{-1}). For releases at non-permissive temperatures, we exposed cells to 37 °C for 30 min before transfer to fresh media (also at 37 °C). Metaphase arrests using nocodazole were done by incubating cells for 3 h with 15 μg ml^{-1} nocodazole. Growth, arrest and release conditions and the concentration of drugs used for every experiment shown are explained in the figure legends. For segregation experiments, *cdc14-1* cells were grown at 25 °C in 2% glucose before shifting the temperature to 37 °C for 2 h to inactivate Cdc14. *cdc14-1* cells arrested in telophase were treated with 66 μg ml^{-1} α-amanitin or kept untreated for 2 h.

Cell extracts and western blotting. To make protein extracts, cell cultures were centrifuged and resuspended in 20 μl of RIPA buffer (10 mM sodium phosphate, 1% Triton X-100, 0.1% SDS, 10 mM EDTA and 150 mM NaCl at pH 7). Cells were physically broken using glass beads in a Fast Prep disruptor machine (2 pulses, 20 s each). The total cell extract was recovered by washing the beads with 200 μl of RIPA buffer. The soluble proteins were obtained by centrifugation for 5 min at 12.000 r.p.m. (Eppendorff 5415D rotor) at 4 °C. Protein concentrations were measured using the BCA protein assay (Sigma). For SDS gels, 30 μg of total cell extract was loaded in 8% polyacrylamide gels in Tris/glycine buffer (3 g l^{-1} Tris, 14.4 g l^{-1} glycine and 1 g l^{-1} SDS). Following gel runs at 30 mA, proteins were transferred to Hybond-P membranes (Amersham-Bioscience) in Tris/glycine buffer without SDS. Membranes were blocked with 5% milk or BSA in PBS with 0.1% Tween-20 (Sigma). Addition of the primary antibodies was as follows: phosphoS2 was used at a concentration of 1:1,000 (provided by D. Eick), H5 antiphosphoS2 (Abcam-24758) was used at a concentration of 1:5,000, phosphoS5 antibody was used at a concentration of 1:5,000, and BSA was used as a blocking agent. Following primary antibody incubation, membranes were washed (1 × 15 min and 2 × 5 min) with PBS/Tween. Secondary antibodies were added at a 1:20,000 concentration. Following incubation with secondary antibody, membranes were washed (1 × 20 min, 2 × 5 min) with PBS/Tween and (2 × 10 min) with PBS. Membranes were incubated with ECL Plus western blotting detection system (Amersham Bioscience) and developed using BioMax MR films (Kodak).

Protein expression and purification. Yeast Rpb1–9×Myc (RNAP-II from yeast) was purified from 10 mg of whole-cell extract using magnetic beads pre-bound with anti-MYC antibodies (μ MACS c-myc; Miltenyi Biotec) following the recommendations of the kit. hRPB1 (RNAP-II from human cells) was purified using 10 mg of whole-cell extract from HEK293T cultures with an antibody against total RNAP-II (H224, Santa Cruz, Sc-9001). Yeast Ssu72, Pph21, Msg5 and Cdc14 and hCDC14A as well as its phosphatase-inactive form were expressed and purified from *Escherichia coli* cultures carrying the expression plasmids. A litre of bacterial cells were grown overnight (50 ml of lysogeny broth plus ampicillin) at 37 °C, to reach $A_{600\,nm}$ of 1.0. Cells were then induced with 0.5 M IPTG for 6 h. Following centrifugation, the pellet was resuspended in 30 ml lysis buffer (0.1% Triton X-100, PBS and 1 mg ml^{-1} lysozyme) and incubated at room temperature for 15 min. Cells were sonicated three times for 30 s on ice, the extract was centrifuged at 14,000 r.p.m. for 30 min and the supernatant was collected. The supernatant was further incubated with 1 ml pre-equilibrated GST beads for 30 min at room temperature, centrifuged and washed three times with 5 ml lysis buffer, then twice with 5 ml lysis buffer plus 0.5 M NaCl and Triton X-100, followed by a final set of three washes with 5 ml lysis buffer. Elution was done by incubation with 5 ml of glutathione for 5 min.

Phosphatase *in vitro* assay. Yeast Rpb1 was incubated with either Ssu72, Pph21, Mgs5, Cdc14 or Cdc14^{CS} purified proteins for 45 min at 30 °C in phosphatase buffer (25 mM HEPES, 150 mM NaCl, 0.1 mg ml^{-1} BSA and 2 mM $MnCl_2$). Human RPB1 was incubated with CDC14A/CDC14A^{CS} for 45 min at 30 °C in phosphatase buffer (25 mM HEPES, 150 mM NaCl, 0.1 mg ml^{-1} BSA and 2 mM $MnCl_2$).

Chromatin immunoprecipitation. Standard chromatin immunoprecipitation (ChIP) was carried out with modifications as follows. Yeast cultures (50 ml) were grown to $A_{600\,nm}$ 0.5. Cells were crosslinked with 1% folmaldehyde for 15 min at room temperature, then glycine was added to 125 mM, cells were centrifuged, washed with PBS and stored at −80 °C. Cells were resuspended in 100 μl immunoprecipitation lysis buffer containing protease inhibitors and 1 mM phenylmethyl sulphonyl fluoride, then subjected to bead-beating. After recovery of spheroplasts, the ChIP protocol was continued as described previously[2]. SYBR Green rtPCR was used for quantification. Primer sequences are available on request. ChIP values were calculated as a percentage of material immunoprecipitated (ChIP/input). The data are presented as a fold enrichment setting the percentage of immunoprecipitated material in the control to 1 (*CEN4* or *ACT1*). All statistical calculations were carried out using the GraphPad PRISM Version 5 statistical software package. A list of primers used for this study can be found in Supplementary Table S2.

Microscopy and determination of segregation defects. Yeast cells with GFP-tagged proteins were analysed by fluorescence microscopy after DAPI or propidium iodide staining. Images were collected on a Leica IRB using a Hamamatsu C4742-95 digital camera and OpenLab software (Improvision). Imaging was done in antifade medium (Molecular Probes) at room temperature. In each chromosome tag segregation/separation experiment an average of 200 cells were counted for each time point and condition.

RNA methods. For total RNA isolation, the cell extracts were cleaned from proteins and DNA using TRIZOL reagent (Invitrogen). Then the RNeasy Kit (Quiagen) was used following the manufacturer's instructions to ensure the total degradation of DNA in the sample. The ThermoScript rtPCR System for First-Strand cDNA Synthesis (Invitrogen) was used. Quantifications were done using SYBR Green rtPCR. Primer sequences are available on request. All statistical calculations (including *P*-value calculations) were carried out using the GraphPad PRISM Version 5 statistical software package.

Microarray transcription analysis. The arrays used were from Affymetrix (PN 520055). Total RNA was isolated by hot phenol extraction. Three replicate hybridizations (biological) of total RNA were carried out. Probe sequences were aligned to the genome sequence of *Saccharomyces cerevisiae* strain S288c. The Affymetrix, Tiling Analysis Software application was used for exploratory data analysis (MVA plots and histograms) and to generate intensities and *P* values. Yeast tiling array cel files were uploaded and normalized with quantile normalization and intensity scaling. Intensity analysis was used to output the relative signal intensities on a −10 log 10 scale and the corresponding *P* values were calculated with a two-sided test. The *P* values were adjusted for multiple testing with the Benjamini–Hochberg method in the R package p.adjust. Perl scripts were written to convert the signals and adjusted *P* values into bigwig format for visualization on the UCSC genome browser. Parteck Genomic suite was used for exploratory data analysis (PCA plots) and to output the raw signal values for the control and treatment groups. The cel files were uploaded and normalized with quantile normalization and RMA background correction. The tiling array data have been deposited in the Gene Expression Omnibus database under the number GSE31020 (http://www.ncbi.nlm.nih.gov/geo/query/acc.cgi?acc=GSE31020).

nature cell biology

DOI: 10.1038/ncb2365

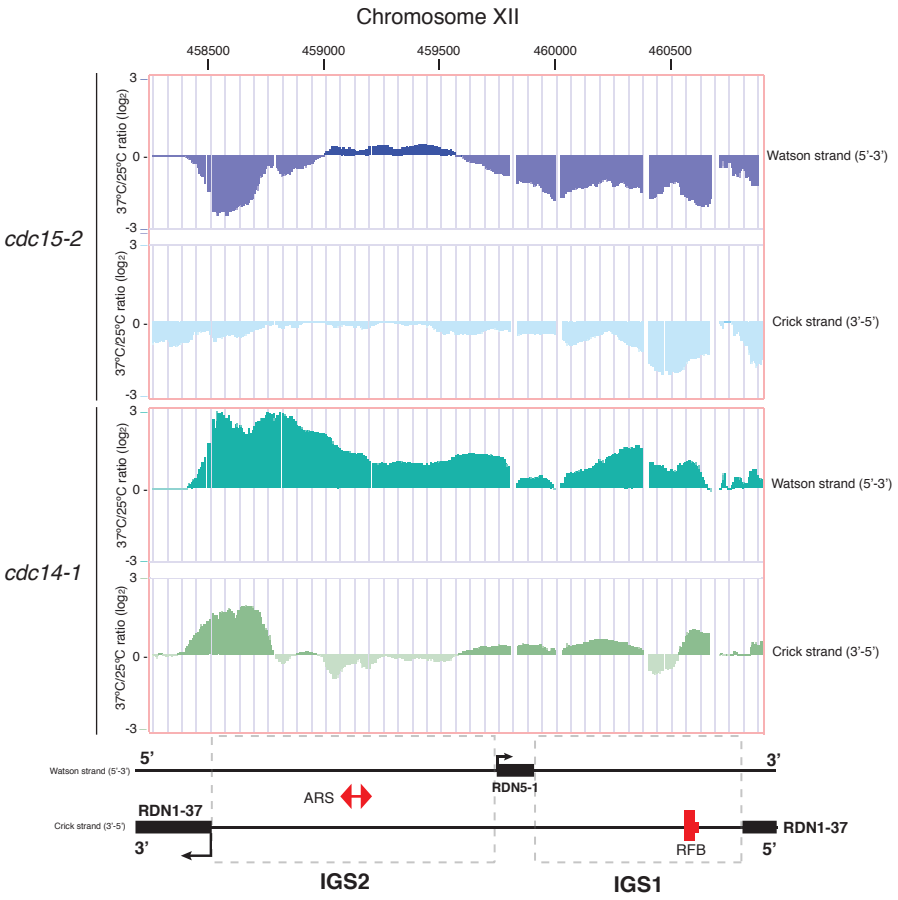

Figure S1 Cdc14 is required for rDNA silencing. Yeast tiling array intensities along 5kb of chromosome XII containing IGS regions (IGS1 and IGS2) (*x* axis). Plotted is the $\log_2$ ratio of transcript abundance in *cdc15-2* (blue) and *cdc14-1* (green) at 37ºC relative to 25ºC for the Watson and Crick strands (*y* axis).

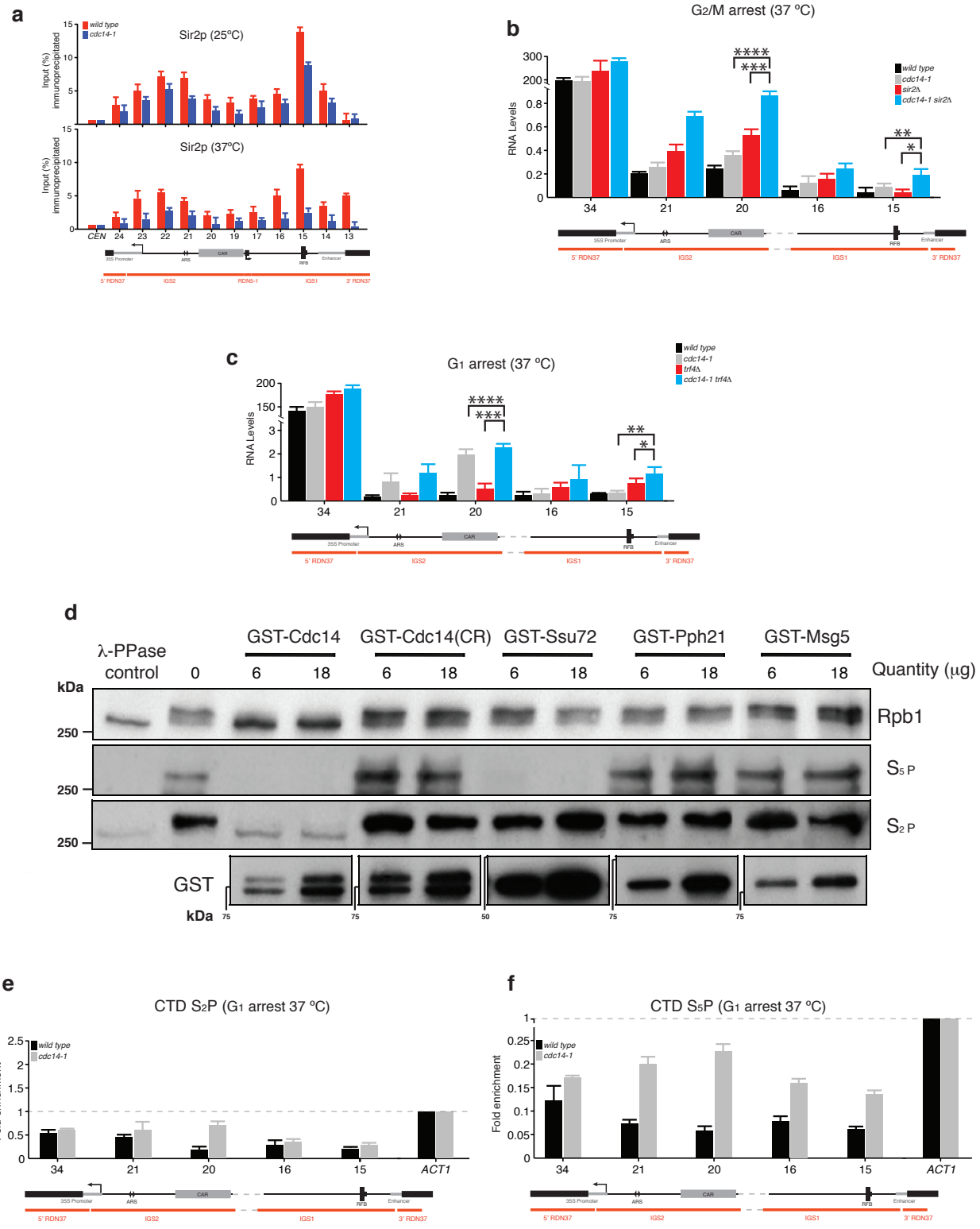

Figure S2 Transcription of sub-telomeric regions lacking Y' elements are unaffected by Cdc14 inactivation. Yeast tiling array intensities along 4 kb of the left telomere region of chromosome XV (*x* axis), which does not contain Y' elements. Plotted is the $\log_2$ ratio of transcript abundance in *cdc14-1*relative to *cdc15-2* at 25ºC (blue) and 37ºC (red) for the Watson and Crick strands (*y* axis).

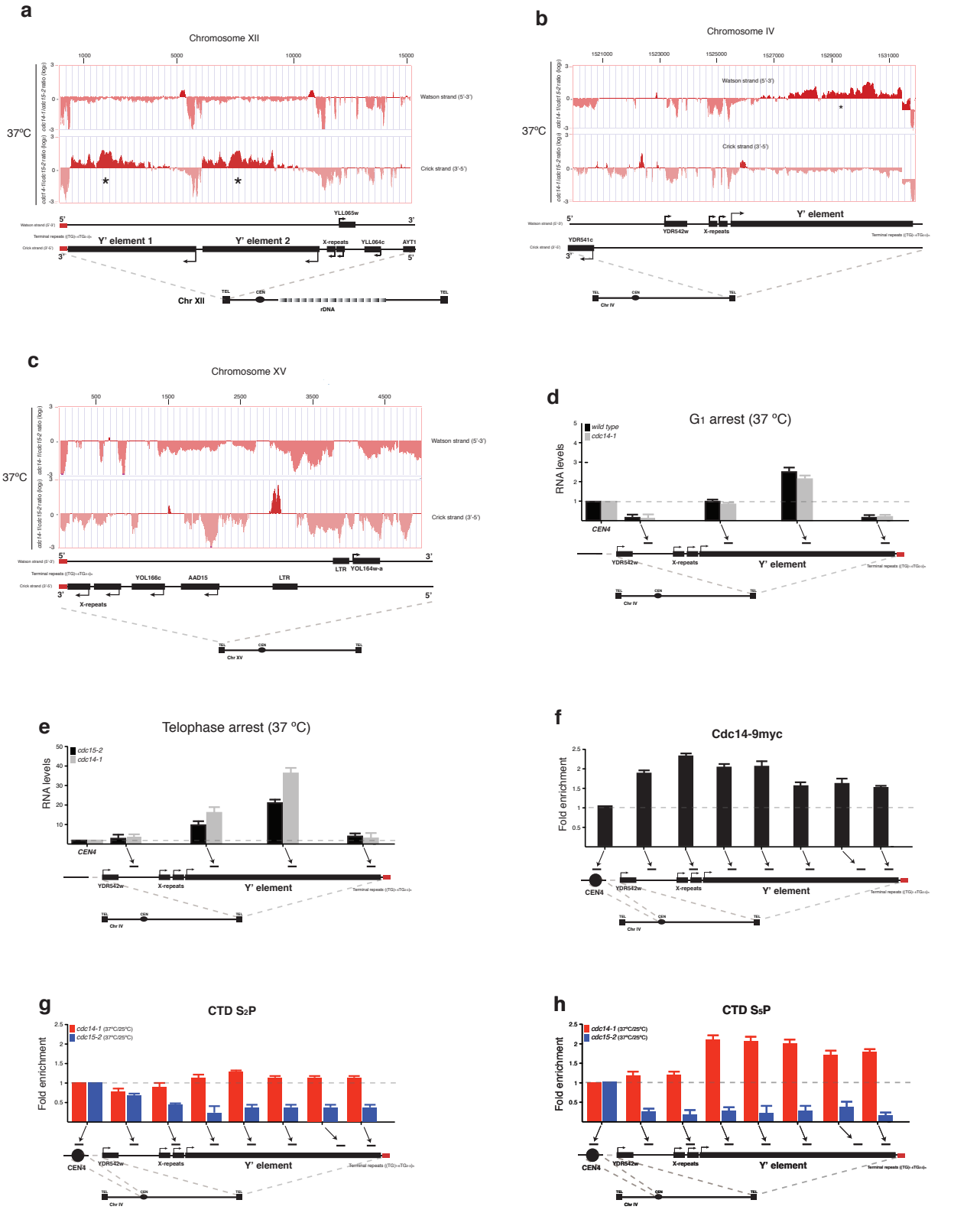

Figure S3 Transcription up-regulation of sub-telomeric Y' elements is caused by Cdc14 inactivation. Yeast tiling array intensities of the distal 15kb of the left telomere of chromosome XII containing two Y' elements (*x* axis). Plotted is the $\log_2$ ratio of transcript abundance in *cdc15-2* (blue) and *cdc14-1* (red) at 37ºC relative to 25ºC for the Watson and Crick strands (*y* axis). Y' elements are indicated (*).

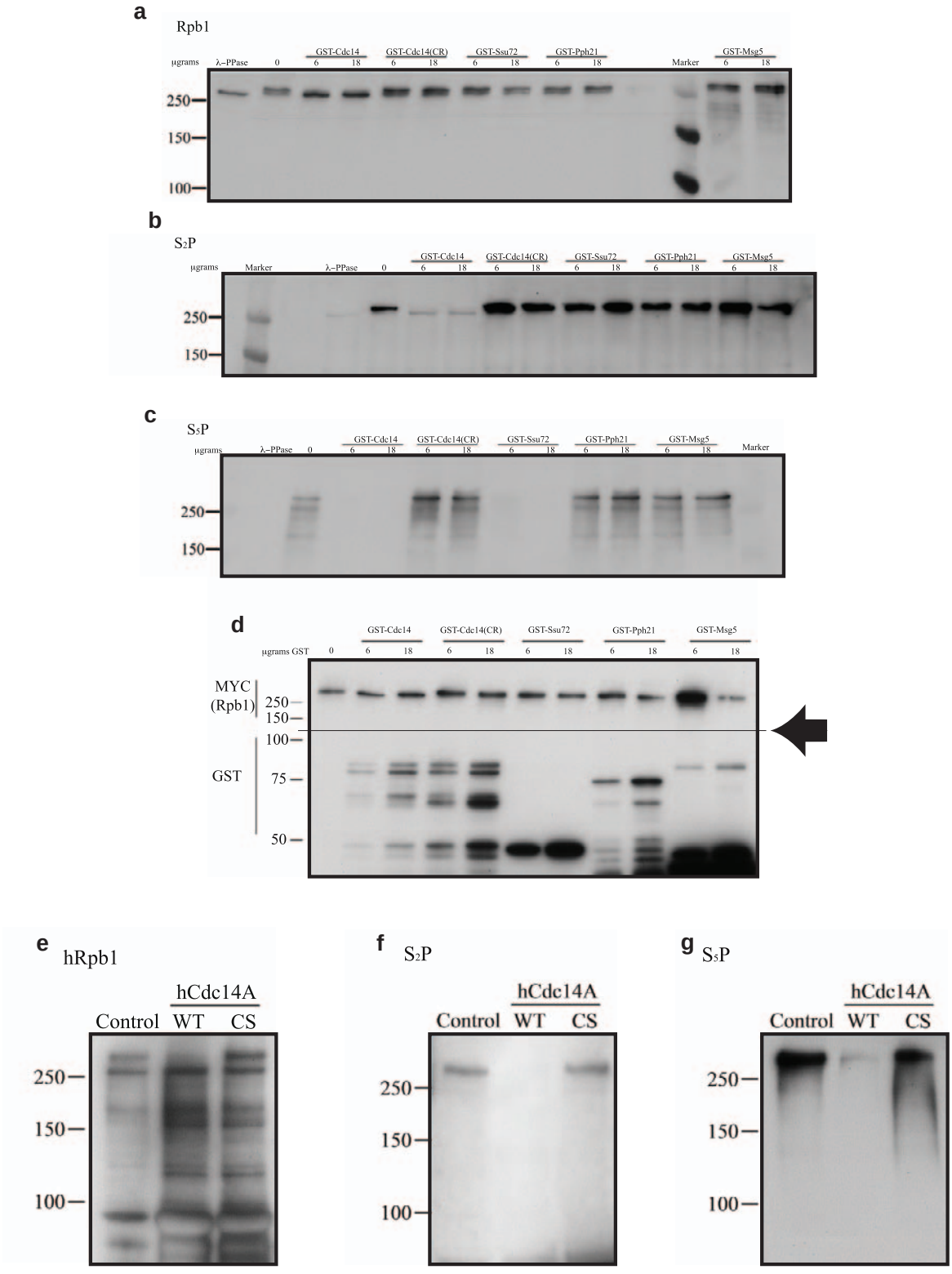

Figure S4 Top-bottom gels of cropped immunoblots. (a), (b) and (c) Phosphatase assays on yeast Rpb1 using a variety of phosphatases as shown and antibodies against myc (a), CTD serine 2 phosphorylation (b), CTD serine 5 phosphorylation (c). Corresponds to Fig. 2d. (d) Validation of GST-quantities added to the in vitro reactions. Note that the gel was cut into two, one half was visualised with antibodies against GST (bottom half as indicated), the other half with myc to confirm presence of the Rpb1 substrate (top half as indicated) in the reaction. Corresponds to GST blot of Fig. 2d. (e) (f) and (g) Phosphatase assays on human Rpb1 using hCDC14A and hCDC14ACS and antibodies against human Rpb1 (e), CTD serine 2 phosphorylation (f), CTD serine 5 phosphorylation (g). Corresponds to Fig. 5c.

Supplementary Materials

Table S1. Yeast strains used

Strain	Relevant genotype	Reference
CCG807	*MATa bar1Δ leu2-3,112 ura3-52 his3-Δ200 trp1-Δ63 ade2-1 lys2-801 pep4 SMC2-3HA LEU2 CDC14-9myc*	L. Aragón
CCG1412	*MATa cdc14-1 leu2 ura3 his3 trp1 ade2 bar1::natMX4*	L. Aragón
CCG1835	**MATa** *bar1:hisG ura3-1 trp1-1 leu2-3,112 his3-11 ade2-1 can1-100 GAL+ cdc15-2*	L. Aragón
CCG3028	*MATa bar1Δ leu2-3,112 ura3-52 his3-Δ200 trp1-Δ63 ade2-1 lys2-801 pep4 TetR-YFP ADE2 TetO(5.6Kb):487Kb ChrXII HIS3 sir2::KanMX4; cdc14-1:9myc:TRP1*	L. Aragón
CCG4000	*MATa bar1Δ leu2-3,112 ura3-52 his3-Δ200 trp1-Δ63 ade2-1 lys2-801 pep4*	L. Aragón
CCG4748	*MATa leu2 ura3 his3 trp1 ade2 lys2 bar1 pep4:HIS3 sir2::KanMX4*	L. Aragón
CCG5315	*MATa bar1Δ leu2-3,112 ura3-52 his3-Δ200 trp1-Δ63 ade2-1 lys2-801 pep4 sir2Δ KanMX4*	This study
CCG5499	*MATa bar1Δ leu2-3,112 ura3-52 his3-Δ200 trp1-Δ63 ade2-1 lys2-801 pep4 CDC14-GPF Kan; TUB4-CFP TRP; NET1-CFP Hyg:MX4; GalCDC20::NatMX4*	This study
CCG6323	*MATa; his3Δ1; leu2Δ0; met15Δ0; ura3Δ0; trf4::kanMX4*	This study
CCG7763	*MATa bar1Δ leu2-3,112 ura3-52 his3-Δ200 trp1-Δ63 ade2-1 lys2-801 pep4 RPB1:9myc KanMX4*	This study
CCG8001	*MATa bar1Δ leu2-3,112 ura3-52 his3-Δ200 trp1-Δ63 ade2-1 lys2-801 pep4 GAL-CDC14 URA3*	This study
CCG8359	*MATa cdc14-1 bar1Δ leu2-3,112 ura3-52 his3-Δ200 trp1-Δ63 ade2::ADE2 tetR-GFP lys2-801 pep4 PRP3:(Tel-IV left):tetO113:URA3 (ARM2-dot)*	This study
CCG8361	*MATa cdc14-1 bar1Δ leu2-3,112 ura3-52 his3-Δ200 trp1-Δ63 ade2::ADE2 tetR-GFP lys2-801 pep4 RAD55:(CEN4 left):tetO113:URA3 (CEN4-dot)*	This study
CCG8362	*MATa cdc14-1 bar1Δ leu2-3,112 ura3-52 his3-Δ200 trp1-Δ63 ade2::ADE2 tetR-GFP lys2-801 pep4 ARS430:(MiddlChrm IV):tetO113:URA3 (ARM1-dot)*	This study
CCG8743	*MATα cdc14-1 leu2 ura3 his3 trp1 ade2 bar1::natMX4*	This study
CCG9249	*MATa cdc14-1 bar1Δ leu2-3,112 ura3-52 his3-Δ200 trp1-Δ63 ade2::ADE2 tetR-GFP lys2-801 pep4 chrmIV:1513kb:(Telomere IV):tetO113:URA3 (TEL4R-dot)*	This study
CCG9328	*MATa, trf4::KanMX, cdc14-1, ADE1, his1, LEU2, TRP1, ura3*	This study
CCG9335	*MATa, leu2, ura3, his3, trp1, ade2, lys2, bar1, pep4:HIS3, SMC2-6HA::KanMX*	This study
CCG9344	*MATa, cdc14-1, leu2, ura3, his3, trp1, ade2, SMC2-6HA::KanMX*	This study
CCG9389	*MATa cdc14-1 bar1Δ leu2-3,112 ura3-52 his3-Δ200 trp1-Δ63 ade2::ADE2 tetR-GFP lys2-801 pep4 chrmIV:15kb:(Telomere IV):tetO113:URA3 (TEL4L-dot)*	This study

Table S2. Primers used in this study.

	rDNA	
rDNA-1-F	TTTGAATGAACCATCGCCAGC	
rDNA-1-R	GATCCTGCCAGTAGTCATATG	Pair 34
rDNA-2-F	TTTCCCACCTATTCCCTCTTG	
rDNA-2-R	CTTCAAGTGTAACCTCCTCTC	Pair24
rDNA-3-F	GGCTATTCAACAAGGCATTCC	
rDNA-3-R	TGTAAATGGCCTCGTCAAACG	Pair 23
rDNA-4-F	AGCCTACTCGAATTCGTTTCC	
rDNA-4-R	ATAGTGAGGAACTGGGTTACC	Pair 22
rDNA-5-F	GGAAGCGGAAAATACGGAAAC	
rDNA-5-R	TCTGAAGCGTATTTCCGTCAC	Pair 21
rDNA-6-F	ATTTCCGCACCTTTTCCTCTG	
rDNA-6-F	AAGACAAATGGATGGTGGCAG	Pair 20
rDNA-7-F	ACCTGTCACCTTGAAACTACC	
rDNA-7-R	AACGGAAACGCAGGTGATATG	Pair 19
rDNA-8-F	GCCATATCTACCAGAAAGCAC	
rDNA-8-R	TCTTCAGAAGAAGAGTGCAGC	Pair 17
rDNA-9-F	CCATTATGCTCATTGGGTTGC	
rDNA-9-R	AGTAAATTTTTGGCGACGCGG	Pair 16
rDNA-10-f	TCGCCAACCATTCCATATCTG	
rDNA-10-R	TTTTTTCCGCACCATCAGAGC	Pair 15
rDNA-11-F	CTCTGATGGTGCGGAAAAAAC	
rDNA-11-R	TCTTTCTAAGTGGGTACTGGC	Pair 14
rDNA-12-F	AGGCTTAATCTCAGCAGATCG	
rDNA-12-R	ATTGGTTTTTGCGGCTGTCTG	Pair 13
	Telomeres	
Tel04R-1-F	CGAGTTACAAGTCATGGTACC	
Tel04R-1-R	ACAAGACGATACGGTGATAGG	Pair1
Tel04R-2-F	TGCTGGATGGTGTTAGACAAG	
Tel04R-2-R	TATTAGGTATACGACCTCGCG	Pair2
Tel04R-4-F	TGGGATTTGAGGATCCAGATC	
Tel04R-4-R	TGAACGGAATGATTGGCCATG	Pair4
Tel04R-6-F	AATGTGGCCCCTGTAAGAAAC	
Tel04R-6-R	CTGTGCCGCTCAAAAAGATTG	Pair6
Tel04R-8-F	AAAAAACAGTTGGGCGGCAAG	
Tel04R-8-R	TATTGCTCTCCTGGAAGCTAG	Pair8
Tel04R-10-F	AGAGTCGTATAAGCGGAAAGG	
Tel04R-10-R	CTCCGATACGATACTTTCTGG	Pair10
Tel04R-12-F	ATCTAAAGTGCCGCATTGGAC	
Tel04R-12-R	TTCACTCTCCAACTTCTCTGC	Pair12
	Controls	
CEN4-R	TTACTGTAAAACTGTGACGATAAAACCG	
CEN4-F	TTTCAGAATGTATGTCCATGATTCGCCGG	
ACT1-R	TTGCATTTCTTGTTCGAAGTCCA	
ACT1-F	GGTATTGTTTTGGATTCCGGTGA	